Decomposing fear perception: A combination of psychophysics and neurometric modeling of fear perception

Article *in* Neuropsychologia · August 2016

DOI: 10.1016/j.neuropsychologia.2016.08.018

CITATIONS
0

READS
82

5 authors, including:

Wen Li
Florida State University
37 PUBLICATIONS **1,425** CITATIONS

SEE PROFILE

Neuropsychologia 91 (2016) 254–261

Contents lists available at ScienceDirect

Neuropsychologia

journal homepage: www.elsevier.com/locate/neuropsychologia

Decomposing fear perception: A combination of psychophysics and neurometric modeling of fear perception

Emily C. Forscher [a,1], Yan Zheng [b,1], Zijun Ke [c,1], Jonathan Folstein [b], Wen Li [b,*]

[a] Department of Psychology, University of Wisconsin-Madison, Madison 53706, USA
[b] Department of Psychology, Florida State University, Tallahassee 32303, USA
[c] Department of Psychology, Sun Yat-sen University, Guangzhou 510275, China

ARTICLE INFO

Article history:
Received 3 May 2016
Received in revised form
16 August 2016
Accepted 17 August 2016
Available online 18 August 2016

Keywords:
Fear perception
ERPs
Psychophysics
Neurometrics
Model fitting

ABSTRACT

Emotion perception is known to involve multiple operations and waves of analysis, but specific nature of these processes remains poorly understood. Combining psychophysical testing and neurometric analysis of event-related potentials (ERPs) in a fear detection task with parametrically varied fear intensities ($N=45$), we sought to elucidate key processes in fear perception. Building on psychophysics marking fear perception thresholds, our neurometric model fitting identified several putative operations and stages: four key processes arose in sequence following face presentation – fear-neutral categorization (P1 at 100 ms), fear detection (P300 at 320 ms), valuation (early subcomponent of the late positive potential/LPP at 400–500 ms) and conscious awareness (late subcomponent LPP at 500–600 ms). Furthermore, within-subject brain-behavior association suggests that initial emotion categorization was mandatory and detached from behavior whereas valuation and conscious awareness directly impacted behavioral outcome (explaining 17% and 31% of the total variance, respectively). The current study thus reveals the chronometry of fear perception, ascribing psychological meaning to distinct underlying processes. The combination of early categorization and late valuation of fear reconciles conflicting (categorical versus dimensional) emotion accounts, lending support to a hybrid model. Importantly, future research could specifically interrogate these psychological processes in various behaviors and psychopathologies (e.g., anxiety and depression).

1. Introduction

Perception organizes and translates multifarious information from the external world and internal milieu into diverse subjective experiences (i.e., percepts). Primary processes of perception involve object detection and recognition, accompanied often by conscious awareness of the object (Schacter et al., 2011). Daily, emotion perception enables detection, categorization, valuation and conscious awareness of emotions such that we effortlessly detect the joy in a child's face or recognize the pain in a wounded soldier, not only the presence but also the quality and strength of the emotions. Yet, how emotion perception is achieved remains a central question in affective sciences.

It is posited that emotion perception involves a complex system consisting of multiple processes and stages (Adolphs, 2002; LeDoux, 1995; Vuilleumier and Pourtois, 2007) mediated by distributed, parallel neural pathways (Pessoa and Adolphs, 2010). The amygdala is known to play a critical role in emotion detection (LeDoux, 2014; Ohman, 2005; Tamietto and de Gelder, 2010; Maren, 2016) and categorization (Adolphs, 2002; Harris et al., 2012b and, 2014). Additionally, the orbitofrontal cortex (OFC) underpins the evaluation of emotional (reward or threat) value of a stimulus (O'Neill and Schultz, 2010; Rushworth et al., 2012; Schultz, 2000), while the medial prefrontal cortex contributes to the conscious awareness of emotion (Amting et al., 2010; LeDoux, 2015; Mitchell and Greening, 2012; Tamietto and de Gelder, 2010). Importantly, outputs from the amygdala and OFC contribute to emotion perception via feedback projections to the sensory cortex (e.g., the ventral visual stream), culminating in emotional percepts of presence (objective or subjective), category (discrete emotions or valence and arousal) and intensity of emotion (Barrett and Bar, 2009; Chikazoe et al., 2014; Phelps and LeDoux, 2005; Vuilleumier and Pourtois, 2007).

Akin to the notion of multiple waves of processing, electrophysiological (mainly, event-related potential/ERP) research of

* Correspondence to: Department of Psychology, Florida State University, B342 PDB, 1107 W. Call St., Tallahassee, FL 32303, USA.
E-mail address: wenli@psy.fsu.edu (W. Li).
[1] These authors contributed equally to the study.

http://dx.doi.org/10.1016/j.neuropsychologia.2016.08.018
0028-3932/

emotion has delineated the time course, arriving at a general consensus of three temporal stages of emotion processing (Adolphs, 2002; Luo et al., 2010). Firstly, indexed by the P1 component (~100 ms), visual sensory processing of emotional stimuli takes place in the occipital cortex (< 120 ms; mediated by subcortical pathways, including fast relays to the amygdala and the prefrontal cortex). Secondly, indexed by the N1/N170 components (~170 ms), the second stage entails intermediate, configural perceptual analysis in the temporal visual cortex. Thirdly, indexed by the P3/P300 and late positive potential (LPP) components (~300 ms and beyond, reflecting high-level, cognitive and motivational processes), emotion perception enters the stage of knowledge-based, goal-oriented processes that often culminate in conscious awareness and volition (cf. Miskovic and Keil, 2012; Olofsson et al., 2008; Vuilleumier and Pourtois, 2007).

However, in comparison to neuroimaging evidence, these ERP findings are not explicitly informative of the particular psychological processes (i.e., emotion detection, categorization, valuation and conscious awareness) involved in emotion perception. Barring convincing evidence that conscious awareness arrives at a later stage of information processing (Del Cul et al., 2007), temporal profiles of the other perceptual processes remain obscure. For instance, theories and extant data have provided opposite conjectures as to whether categorization would arise early, even in the initial sensory feedforward sweep, or late, following more basic processes such as detection (Young et al., 1997; Mathews and Mackintosh, 1998; Riesenhubger and Poggio, 1999; Serre et al., 2007; Brosch et al., 2010).

Here, combining psychophysical testing and neurometric analysis, we took a data-driven approach to delineate the temporal profiles of primary psychological processes in fear perception and assess their contribution to behavioral outcome in a fear detection task. We parametrically manipulated fear intensity using morphed images of fearful facial expressions (Fig. 1A and B). While assessing the psychophysical function of fear detection, we mapped ERP responses to varying levels of fear to neurometric models associated with four key processes of emotion perception (Fig. 1C).

Akin to signal detection, fear detection was modeled with a sigmoid function. Given the widely present sensitivity to threat (even at minimal levels) across species including humans (Forscher and Li, 2012; Helfman, 1989), we predicted that the related ERP response would quickly arise and asymptote as soon as a faintly fearful face became psychologically distinct from its neutral morph, conforming largely to the upper half of a sigmoid curve. The process of emotion categorization (classifying faces into neutral and fearful categories) was modeled by an upward quadratic function, depicting maximal ERP magnitude at prototype levels of fearful and neutral expressions and minimal magnitude at the category boundary (i.e., midpoint between the two prototypes; Goldstone and Hendrickson, 2010). The process of fear valuation (encoding fear intensity) was modeled to a linear function between ERP magnitude and fear intensity (i.e., tracking the physical distance of fear morphing percentages). Lastly, the process of conscious awareness of fear was modeled by a sigmoid function (Del Cul et al., 2007). In contrast to the sigmoid function of fear detection, we expected a low response asymptote that persisted at low to intermediate fear levels until a sharp rise at a high fear level commensurate with conscious perception in the viewer.

2. Methods

2.1. Participants

Forty-five undergraduate students of the University of Wisconsin-Madison (25 female; mean age 20 ± 4 years) participated in the study. All students were right-handed, with normal or corrected-to-normal vision, no history of neuropsychological problems, and no current use of psychotropic medications. Participants provided informed consent to take part in the study, which was approved by the University of Wisconsin Institutional Review Board. Three participants with excessive EEG interference and artifacts were excluded from ERP analyses.

2.2. Stimuli

Pictures of 7 models (3 female) expressing fearful and neutral expressions were selected from the Karolinska Directed Emotional Faces (KDEF; Lundqvist et al., 1998). All images were frontal views, in color and with a consistent background. Fearful and neutral pictures of each model were then morphed together using FantaMorph (Abrosoft, Beijing, China) on a continuum of 0% (pure neutral) to 100% (pure fearful) to create graded fearful expressions (Forscher and Li, 2012). We parametrically varied fear intensity at

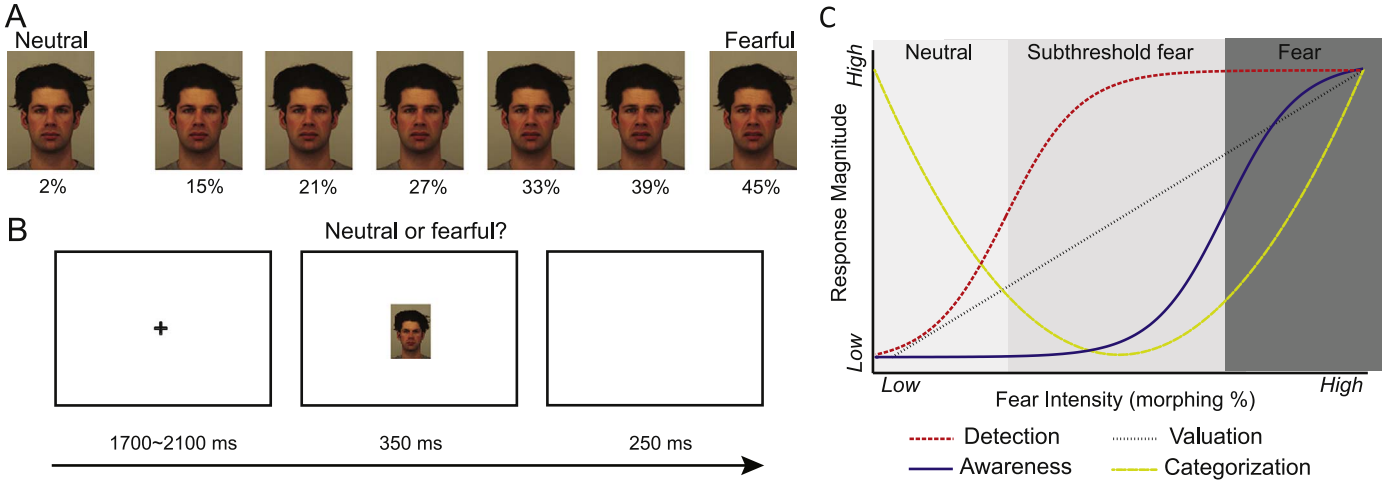

Fig. 1. *Experimental paradigm and neurometric hypotheses.* (A) Example stimuli with the neutral prototype (at 2% of the neutral-fear morph continuum) and the six fear levels (15–45% in 6% increments). A total of 686 trials (98 trials per morph level) was randomly presented in four blocks. (B) Participants performed a fear detection task: Following a jittered interval, a face appeared (350 ms) at the center of the screen, to which subjects made a forced choice of "neutral" or "fearful" by button-pressing. (C) The psychological processes in question were modeled according to their psychometric functions. The red sigmoidal curve illustrates the process of fear detection. The yellow quadratic curve illustrates the process of fear-neutral categorization. The gray line illustrates the linear process of fear valuation. Lastly, the blue sigmoidal curve illustrates the process of fear awareness. (For interpretation of the references to color in this figure legend, the reader is referred to the web version of this article.).

6 levels – 15%, 21%, 27%, 33%, 39%, and 45% – with an increment of 6% (Fig. 1B). To include a high number of trials to ensure ERP signal quality, we had to limit the highest level of fear to 45%, which was determined based on systematic piloting to generate reliable and conscious fear detection. For neutral face stimuli, we used a 2% morph to match visual alterations caused by the morphing procedure (Forscher and Li, 2012).

2.3. Procedure

Fear detection task: Participants were seated in a dimly lit, sound-attenuated room, 120 cm from a 20-inch CRT monitor. Each trial began with a fixation cross at the center of the screen for 1700–2100 ms, followed by a face image displayed centrally for 350 ms, to which participants indicated via button press whether they perceived fear in the face (Yes/No response). The face image subtended a visual area of 2.6° by 3.5° (Fig. 1B). A total of 686 trials (98 trials per morph level) was randomly presented in four blocks. Stimulus presentation and response collection were controlled using Cogent2000 software (Wellcome Department of Imaging Neuroscience, UK), implemented in Matlab (MathWorks, MA, USA).

2.4. EEG data acquisition & analysis

EEG was recorded from a 96-channel (ActiveTwo; BioSemi) system at a 1024 Hz sampling rate with a 0.1–100 Hz bandpass filter. Electrooculogram (EOG) was recorded at two eye electrodes at the outer canthi and one electrode infraorbital to the left eye. EEG/EOG signals were then digitally bandpass filtered from 0.1 to 40 Hz, and down-sampled to 256 Hz. Data were then submitted to Fully Automated Statistical Thresholding for EEG Artifact Rejection (FASTER; Nolan et al., 2010) a plug-in function in EEGLAB (Delorme and Makeig, 2004). FASTER first detected deviant channels and interpolated them using the EEGLAB spherical spline interpolation function. Data were then epoched from -200 to 600 ms around face onset, corrected to the 200-ms pre-stimulus baseline. FASTER then automatically detected and rejected deviant epochs with a Z score $> \pm 3$ in amplitude range, variance, and deviation. Data were then re-referenced to averaged mastoids and entered into independent component analysis (ICA) using the Infomax algorithm (Bell and Sejnowski, 1995), which detected and removed artifact-related components. Lastly, one more round of channel rejection and interpolation was performed for each epoch.

To unpack the psychological processes mentioned above, we extracted P1, N170, P300 and LPP components based on the global field power (GFP) waveform (Fig. 3A) and the literature (Miskovic and Keil, 2012; Olofsson et al., 2008; Vuilleumier and Pourtois, 2007). Inspection of the grand average ERP waveform confirmed a P1 component maximal at occipital sites, peaking at 100 ms after face onset. Mean P1 amplitudes were extracted at Oz (collapsed across five electrodes) over a 36-ms interval centered on the peak (peak ± 4 samples, Fig. 3B). An N170 component was identified at occipito-parietal sites (PO7 & PO8; collapsed across five electrodes), peaking at 152`ms after face onset. Mean N170 amplitudes were extracted over a 36-ms interval (peak ± 4 samples) centered on the peak. Finally, two distinct positive peaks were observed, both with centroparietal scalp distributions, which we labeled P300 and LPP. We extracted P300 (270–370 ms, centering on the peak) and LPP mean amplitudes (400–600 ms) at Pz (collapsed across five electrodes), where these components were largest (Fig. 3C). The LPP component encompassed a wide window of 200 ms, and to delve into the temporal progression closely, we divided this component into two 100-ms windows (early and late window for 400–500 ms and 500–600 ms, respectively). This division also accorded with the two distinct peaks for the two 100-ms windows in the GFP waveform (Fig. 3A), and was conceptually consistent with the notion that the LPP reflects a complex potential of P3b and later slow wave potentials (Olofsson et al., 2008).

2.5. Statistical analysis

We conducted one-way repeated measures analyses of variance (ANOVAs; with Greenhouse–Geisser corrections) of fear intensity (morphing %) on fear detection rate and reaction time (RT; RTs beyond ± 3 SD from the individual's mean were excluded). Given the inherent sigmoid relationship between fear intensity levels and fear detection rates, we also fitted the group-level fear detection rates to a sigmoid function using the psignifit toolbox (http://bootstrap-software.org/psignifit/), which implements the maximum-likelihood method described by (Wichmann and Hill, 2001).

We then performed similar one-way ANOVAs of fear intensity on ERP mean amplitudes. Importantly, to test the hypothesized neurometric functions (Fig. 1C), we assessed trend effects (linear and quadratic effects) of fear intensity, in addition to a simple main effect, on the ERP amplitudes. These trend effects, if significant, were followed by curve fitting (based on the group mean; Jemel et al., 2003) of linear, quadratic and sigmoidal fit (Boltzmann fit) in OriginPro (OriginLab, Northampton, MA, USA) to determine their fit to the predicted models (Fig. 1C). Finally, we examined the contribution of the neural and psychological processes to the behavior outcome based on the brain-behavioral association (i.e., within-subject correlation between ERP amplitudes and fear detection rates). The subject-level *r*'s were normalized using Fisher's *Z*-transformation before submission to a *t*-test.

3. Results

3.1. Behavioral results

3.1.1. Fear detection rate

A one-way ANOVA of fear intensity (i.e., morphing %) indicated a strong main effect of fear intensity on fear detection [$F(1.88, 82.51) = 412.33$, $p < .001$]]: fear detection rates [*M (SD)]* were .08 (.11), .14 (.12), .21 (.14), .42 (.16), .61 (.17), .74 (.16), and .85 (.15) for the 7 levels (2–45%). Follow-up paired *t*-tests further revealed significant differences between any two levels (adjusted *p*'s $< .001$; Holm-Bonferroni multiple comparison correction). Notably, trend analysis indicated that both linear and quadratic effects were significant, F's > 12.63, p's $< .001$. As illustrated in Fig. 2A, these trend effects were expressed in a very close fit of a sigmoid function (with a deviance score of .32 and p of .96). Using conventional cutoffs, we set thresholds for suprathreshold/conscious perception of fearful and neutral expressions at 75% and 25% fear detection rates (half way between chance and perfect performance; Klein, 2001; Zwislocki and Relkin, 2001), respectively, with in-between detection rates (25–75%) reflecting subthreshold/unconscious fear perception. According to the fitted sigmoid function, 75% and 25% fear detection rates corresponded to 40.06% and 20.01% morphing percentages, respectively. As such, 45% fear would correspond to suprathreshold (conscious) fear perception (with 39% at the borderline), 27% and 33% to subthreshold (unconscious) fear perception (with 21% at the borderline), and 15% and below to neutral emotion perception (i.e., both the physical neutral/2% fear level and the 15% fear level belonged to the psychological domain of neutral emotion). Lastly, the inflection point (50% detection rate) was located to 30.05% fear, reflecting the psychological category boundary between fear and neutral emotions. These critical levels were applied in the following neurometric analysis.

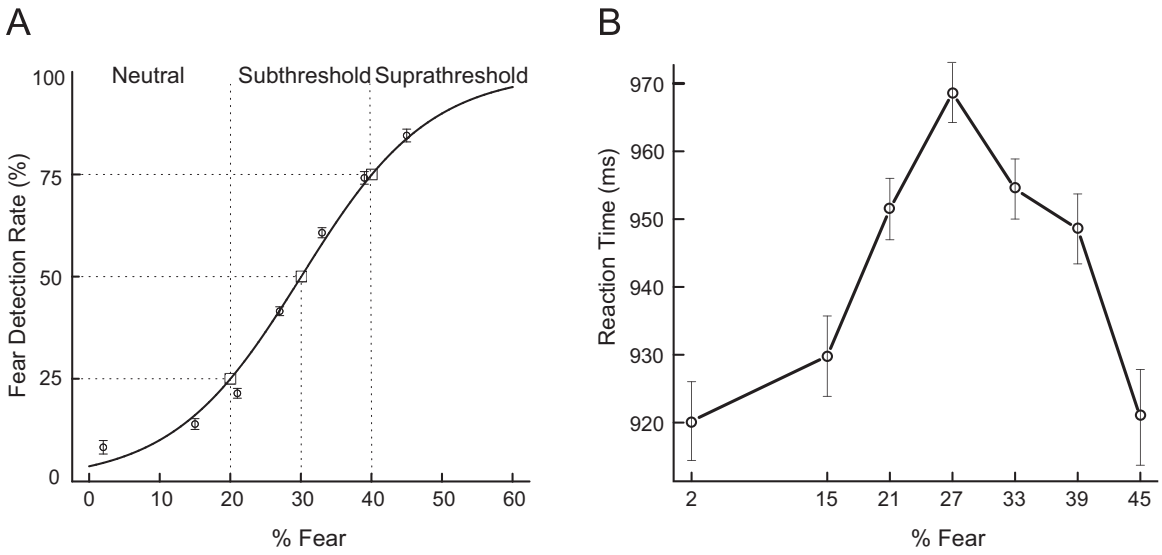

Fig. 2. *Behavior results.* (A) Fear detection rate as a function of fear intensity (indexed by fear morph %). The response pattern fits very tightly to a sigmoid function (solid curve) Estimated based on the sigmoid function, the boxes indicate the thresholds for subthreshold/unconscious (20.01% fear) and suprathreshold/conscious (40.06% fear) fear perception, and the inflection point (30.05% fear). (B) Fear detection reaction time as a function of fear intensity. Error bars indicate individual-mean-adjusted S.E.M. (i.e., S.E.E.).

3.1.2. Reaction time (RT)

A similar one-way ANOVA showed a strong main effect of fear intensity on fear detection RT [F (2.33, 102.40)=10.13, $p<.001$]. Trend analysis further indicated a quadratic [F (1, 44)=46.46, $p<.001$] but not a linear effect ($p=.472$). Consistent with the quadratic effect, the RT pattern conformed to an inverted U shape (Fig. 2B), with the longest RT at 27% fear level [969 (18) ms; presumably the most ambiguous level] and progressively shorter RTs towards the high [33%: 954 (17) ms, 39%: 949 (17) ms, and 45%: 921 (16) ms] and low ends of fear intensity [15%: 930 (16) ms, 21%: 951 (17) ms] and neutral [2%: 920 (16) ms] levels. Notably, differences between 27% fear and all other but 33% fear levels were significant, t (44)'s > 3.14, adjusted p's < .05 (the contrast with 33%, t=2.54, only survived at the uncorrected $p<.05$). Note, 27% and 33% levels are right next to the inflection point of the fitted sigmoid curve (boundary between fear and neutral categories). The RT results thus coincided with the psychophysical sigmoid fit, confirming the fear/neutral emotion category boundary around 30% fear.

3.1.3. ERP results

3.1.3.1. P1 component. A one-way ANOVA showed a marginally significant simple effect of fear intensity on P1 amplitudes [F(3.33, 136.62)=2.25, p=.079], which was expressed in a strong quadratic effect [F(1,41)=10.443, p=.002] but not a linear effect (p=.136; Fig. 3B). Accordingly, the follow-up curve fitting indicated a strong upward quadratic fit (R^2=.75) whereas the sigmoid fit failed (model did not converge after 1000 iterations; Fig. 3D). Consistent with this quadratic fit, P1 was lowest around the category boundary [27% and 33% fear] and higher at the two prototype levels [suprathreshold fear (45%) and neutral emotions (2% and 15%)]. As illustrated in the topographical map (Fig. 3D), there was a strong difference between the prototype and boundary levels (2% and 45% combined minus 27% and 33% combined) at Oz [t(41)= 3.34, p=.001]. Therefore, the P1 response generally aligned with the psychometric function of categorization between neutral and fear emotions.

3.1.3.2. N170 component. A similar one-way ANOVA indicated no significant effect of fear intensity on N170 amplitudes at either PO7 or PO8 (Fs < .95, p's > .45), nor was there a significant linear or quadratic effect (F's < 2.27, p's > .14). Therefore, evidence fails to support fear processing during this stage.

3.1.3.3. P300 component. Although a one-way ANOVA failed to indicate a simple effect of fear intensity on P300 amplitudes [F (4.92, 201.64)=1.41, p=.213], trend analysis revealed a significant linear effect [F(1, 41)=5.26, p=.027] and a marginally significant quadratic trend effect [F(1, 41)=3.71, p=.061; Fig. 3C]. Follow-up curve fitting further indicated that the response pattern was strongly fitted with a sigmoid (R^2=.92) or downward quadratic function (R^2=.92), in comparison to a linear fit (R^2=.63). As illustrated in Fig. 3D, the sigmoid and quadratic curves were highly overlapping. Nuanced follow-up level-wise contrasts further confirmed the sigmoid (vs. quadratic) fit. P300 at levels of 21% and above was significantly higher than 2% fear (p's=.007∼.088) but did not differ among each other (p's > .304). P300 amplitudes at 2% and 15% fear did not differ (p=.187). Namely, P300 was minimal at the physical neutral level (2% fear), sharply increased at 15% and plateaued at 21% fear. Notably, this 21% plateau point coincided with the threshold for subthreshold fear perception (20.01% fear). This response profile thus conformed to the sigmoid curve (vs. the quadratic curve, which predicted a distinct peak response around 33% fear). Overall, the P300 response pattern aligned closely to the predicted neurometric profile of the process of fear detection. We note the R values reported here and below were very high, which nonetheless is not unusual for curve fitting based on the group average (e.g., Jemel et al., 2003). Also, as indicated in the topography (Fig. 3D), these neurometric functions had distinct spatial distributions, helping to exclude the possibility of overfitting. Finally, as individual variability had been considered in the ANOVA, the curve fitting procedure was essentially to qualify the pattern of the trends.

3.1.3.4. Early LPP (eLPP) component. A one-way ANOVA on the eLPP component (400–500 ms) indicated a significant simple effect of fear intensity [F (5.06, 207.43)=9.93, $p<.001$; Fig. 3C]. Trend analysis further revealed a strong linear trend [F (1, 41)=35.16, $p<.001$] but not a quadratic trend (p=.253). Given the lack of a quadratic trend effect, we did not continue with polynomial curve fitting (quadratic or sigmoid). In keeping with the strong linear trend, Fig. 3D illustrates a close linear fit of the response pattern,

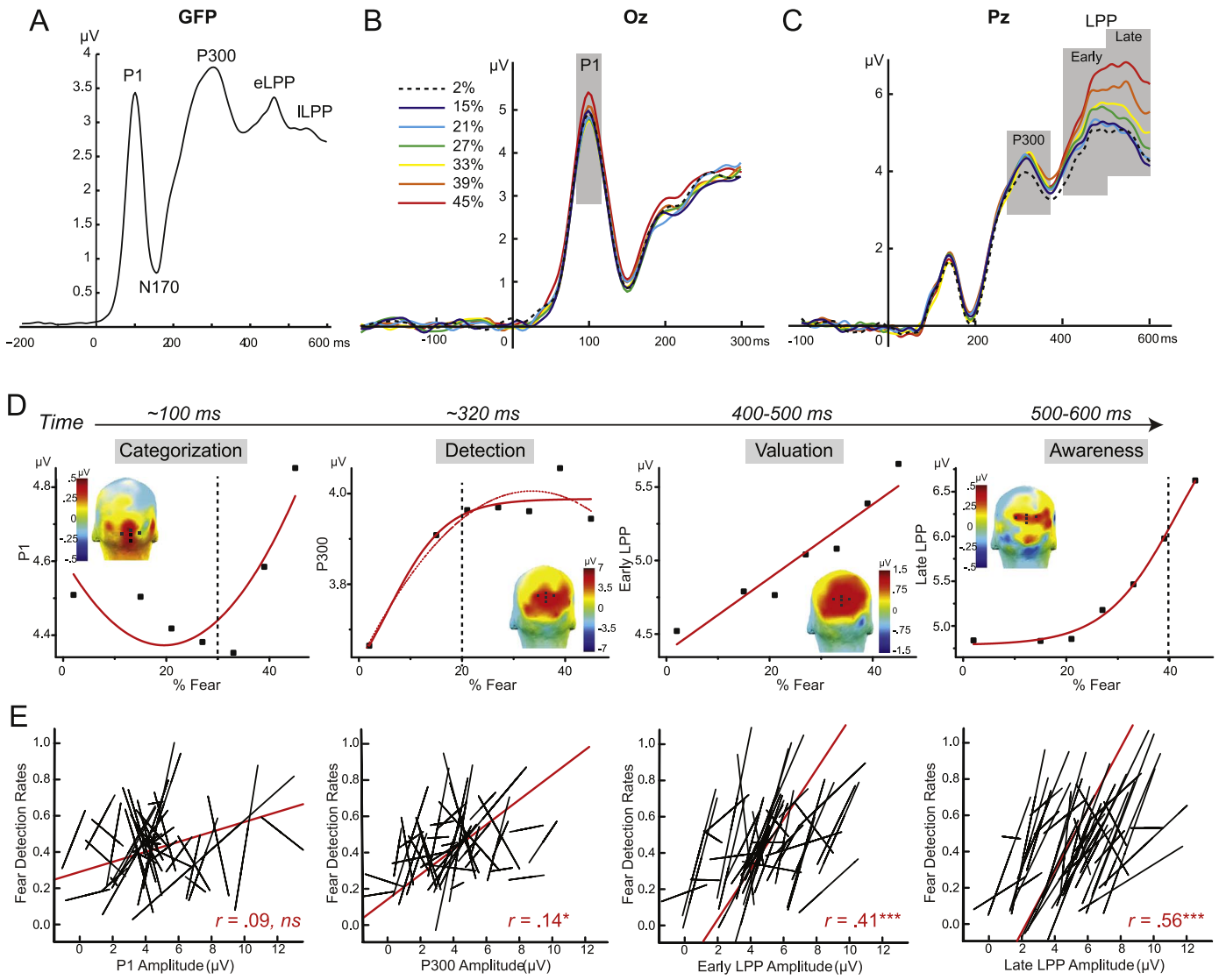

Fig. 3. *ERP results.* Global field power (GFP) waveform shows the main ERPs of interest (A). Grand average ERP waveforms at site Oz (marked by 5 black dots) show P1 potentials (B) and at site Pz (marked by 5 black dots) show P3 and early and late LPP potentials (C) for the neutral and 6 fear levels. (D) Neurometric curve fitting (red curves) reveals key processes emerging over time in sequence. Emotion categorization: P1 amplitudes conformed to an upward quadratic function; topographical map – two prototype levels minus two boundary levels: [(Levels 2%+45%) – (Levels 27%+33%)]/2. Fear detection: P300 amplitudes conformed to a sigmoid function (primarily, upper half; red solid line); topographical map – asymptote minus neutral levels: [average of Levels 21–45% – 2% (neutral level)]. We also show a downward quadratic curve in red dotted line, which was nevertheless not confirmed by follow-up level-wise contrasts. Fear valuation: early LPP (400–500 ms) amplitudes conformed to a linear function; topographical map – a linear trend: 3*Level 45%+2*Level 39%+Level 33% - Level 21%−2*Level 15%−3*Level 2). Fear conscious awareness: late LPP (500–600 ms) amplitudes conformed to a sigmoid function (primarily, lower half); topographical map – suprathreshold minus asymptote levels: [(Levels 45%+39%)/2 – average of Levels 2–33%]. Vertical dotted lines indicate psychophysical cutoffs for 25%, 50% and 75% fear detection. (E) Brain-behavior association – correlation between fear detection rates and ERP amplitudes. Straw plots indicate no correlation for the P1 component, significant but weak correlation for the P3 component, and significant and strong correlation for the two LPP components. Each black line corresponds to the regression line for an individual subject (between ERP amplitudes and fear detection rates); red lines correspond to regression lines for the group. eLPP=early LPP; lLPP=late LPP;*, $p < .05$;***, $p < .001$. (For interpretation of the references to color in this figure legend, the reader is referred to the web version of this article.).

such that the eLPP amplitude tightly tracked fear % ($R^2=.93$). Therefore, the eLPP response pattern conformed to the predicted neurometric profile of fear valuation.

3.1.3.5. Late LPP (lLPP) component. Finally, a one-way ANOVA on the lLPP component (500–600 ms) indicated a significant simple effect of fear intensity [F (3.99, 163.55)=25.45, $p < .001$], expressed in both a strong linear [F (1, 41)=58.15, $p < .001$] and quadratic [F (1, 41)=41.17, $p < .001$; Fig. 3C] trend across the levels. Follow-up curve fitting revealed that the response pattern was best fitted with a sigmoidal function (primarily, the lower half of a sigmoid curve; $R^2=1$; Fig. 3D) although also very well with a downward quadratic function ($R^2=.99$) while a linear fit underperformed in comparison ($R^2=.73$). Moreover, according to the psychophysical cutoff of conscious fear perception (40.06%), we compared 45% and 39% fear levels with all lower fear levels. All t-tests were significant (p's $< .01$ corrected), with the exception of a marginal difference between 39% (borderline level) and 33% ($p=.016$ uncorrected). Taken together, these results suggest that lLPP response pattern matched the predicted neurometric profile of conscious awareness of fear.

3.2. Brain-behavior association

Lastly, to link these processes to behavioral outcome in fear detection, we examined within-subject correlation between ERP amplitude and fear detection rate across the seven fear levels. We note that within-subject correlation directly assesses covariance

between the variables themselves, compared to between-subjects correlation that indirectly reflects association based on between-subjects variability. Submitting the Fisher Z-transformed values of r (Zr) to t-tests, we observed significant positive correlations between fear detection rate and P300, eLPP and lLPP amplitude, r (Zr)=.13 (.16), p=.019; r (Zr)=.41 (.53), $p < .0001$; r (Zr)=.56 (.80), $p < .0001$, respectively (Fig. 3E). No significant correlation was observed for P1 nor N170 potentials [r's < .09, Zr's < .11, p's > .23]. A one-way ANOVA (with the ERP components as the independent variable) indicated a strong effect of ERP component on Zr [F(2.75, 112.88)=20.48, $p < .0001$]. Follow-up contrasts further confirmed that the correlation between fear detection rate and Zr for the eLPP and lLPP was significantly stronger than the other correlations, corrected p's < .001, indicating the especially important contribution of these later processes to fear detection performance.

4. Discussion

Combining psychophysics, brain electrophysiology and neurometric analysis in a fear detection task with parametrically varied fear intensities, we delineated the temporal profiles of four putative processes key to emotion perception. These four psychological processes occurred in sequence following face presentation: (1) swift categorization of fear versus neutral emotion at ~100 ms, (2) detection of fear at ~320 ms, picking up minute but psychologically meaningful signals of fear, (3) valuation of fear signal at 400–500 ms, tracking small physical distances in fear intensity, and lastly (4) conscious awareness of fear at 500–600 ms, supporting visibility of high-level fear.

This temporal evolution exemplifies the well accepted notion of coarse-to-fine progression of emotion processing (LeDoux, 1995; Mathews and Mackintosh, 1998). In relation to the longstanding debate of category (or basic emotion; Ekman, 1992) versus dimension (e.g., circumplex; Russell, 1980) accounts of emotion in the literature, the chronometry highlights categorical perception of emotion at an early stage and dimensional perception at a later stage (Krusemark and Li, 2013; Young et al., 1997), in support of a reconciliatory, hybrid model that incorporates both categorical and dimensional aspects of emotion (Christie and Friedman, 2004; Hamann, 2012; Russell, 2003). By timing the emergence of conscious awareness of fear, we uncover the implicit nature of multiple processes (fear categorization, detection and valuation), underscoring the contribution of unconscious processes in constructing our fear experiences. By ascribing psychological meaning to ERPs elicited by fear stimuli, future research could specifically tackle psychological processes in various behaviors and psychopathologies such as anxiety and depression. Finally, we note that our modeling of the primary ERPs elicited by fearful expressions to key psychological processes purportedly involved in emotion perception does not exclude the fact that these ERPs were also reflective of various information processing operations (e.g., basic feature processing, attention, semantic attribution, etc.).

As indexed by the P1 component, fear processing arises as early as 100 ms after stimulus onset, consistent with extant evidence of rapid emotion processing (even earlier than 100 ms; cf. Miskovic and Keil, 2012; Olofsson et al., 2008; Vuilleumier and Pourtois, 2007). Our neurometric analysis further suggests that this early processing is likely associated with coarse categorization between fearful and neutral facial expressions, characterizing the gist of "threat/fear" versus "neutral" in the faces. The latency of this emotion categorization process concurs with that of standard object categorization (e.g., natural vs. domestic scenes; Thorpe, 2009), purportedly mediated by fast subcortical visual pathways and quick feedback from the prefrontal cortex (Barrett and Bar, 2009). This putative early emotion categorization also accords with the notion that facial expressions, owing to the ecological importance, elicit rapid categorical emotion perception classifying prototypical facial expressions based on automatic, bottom-up sensory input (Brosch et al., 2010; Young et al., 1997). With the intermixed presentation of minutely differing fear intensities, this putative early categorization may reflect typicality processing by coarsely classifying faces based on stimulus typicality (prototypical fearful or neutral facial expressions), thereby reducing the dimensionality of incoming sensory input. This categorization process may thus be prioritized and consequently overshadow or delay preferential processing of fear that can occur during the P1 window with prototypical facial emotions (Brosch et al., 2011; Pourtois et al., 2004). Indeed, the absence of correlation between P1 amplitudes and fear detection rates corroborates the automatic, potentially mandatory nature of early emotion categorization (Krusemark and Li, 2013), which could be rather detached from the behavior outcome.

Akin to its role in face processing and object categorization (Johnson, 2005; Mormann et al., 2011), the amygdala has been implicated as critical for categorical perception of facial expressions (Harris et al., 2012, 2014). It is thus possible that the amygdala quickly extracts emotional categories based on subcortical visual input and then informs emotion categorization in the visual cortex via feedback projections (Barrett and Bar, 2009; Phelps and LeDoux, 2005). Alternatively, as accruing human and animal evidence implicates the sensory cortex for long-term storage of emotion representations, it is worth considering that emotional stimuli activate emotion representations during the initial feedforward sensory sweep, resulting in early emotion categorization (Li, 2014; Li et al., 2008; Miskovic and Keil, 2012; Padmala and Pessoa, 2008; Sacco and Sacchetti, 2010; Weinberger, 2007; You and Li, 2016).

In the subsequent P300 and LPP windows, we observe progressively refined processes that are increasingly linked to behavioral performance. At ~320 ms (the P300 window), the brain seems to enter a detector mode, marking the psychological significance of a threat signal. As the sigmoid curve indicates, this detector has high sensitivity and low specificity: while dismissing neutral or minimally fearful expressions (15%), it recognizes minute fear (21% fear) but does not differentiate fear intensities above this threshold, including the level that engenders conscious fear perception (e.g., 45% fear). Importantly, this detector follows the psychophysical function, with its threshold (21% fear level) matching the psychophysical threshold for unconscious fear perception (20.01% fear; Fig. 2A).

Compared with the swift categorization process, this processing stage may engage a slower cortical relay from the primary visual cortex through the inferotemporal cortex to the amygdala (Amaral et al., 1992), a key region for fear detection (Ohman, 2005; Vuilleumier et al., 2003). Relative to the coarse subcortical pathway responsive to emotion prototypes, this cortical pathway would isolate weak fear signals to support detection of subtle fearful expressions (Breiter et al., 1996; Davis and Whalen, 2001; Morris et al., 1996). Interestingly, we observe a statistically significant but pragmatically insignificant correlation between P300 amplitudes and fear detection rates (accounting for 2% of total variance), suggesting internal decision-making about biological saliency at this stage, to be followed by more elaborate analysis beyond the visual cortex and subcortical structures to generate reliable behavioral output of fear detection.

The ensuing e/lLPP components may provide insights into such higher-order processes contributing directly to behavior. The LPP component is reliably observed in emotion processing and is especially salient for highly charged, emotional stimuli (cf. Olofsson and Polich, 2007; Vuilleumier and Pourtois, 2007). Moreover, LPP amplitudes would vary with emotion/arousal intensity

(Cuthbert et al., 2000a; Keil et al., 2002; Schupp et al., 2000). Here, parametric manipulation of emotional expressions allows a nuanced look into this association: the eLPP linearly tracks the intensity of fearful expressions while the lLPP rises non-linearly with fear intensity. Thus, two distinct operations emerge in this later stage of processing, with the early one (400–500 ms) defining the physical space and the late one (500–600 ms) specifying the psychological space of fear.

Conforming closely to a fear valuator (Fig. 1C), information processing during the eLPP window faithfully encodes the actual spacing between fear intensity levels such that the eLPP increases at a constant rate with increasing fear. Importantly, this process has a tight association with behavior, contributing to 17% of the behavioral performance of fear detection. This fine linear profile aligns with the pattern of OFC valuation of the emotional and motivational value of a stimulus (O'Neill and Schultz, 2010; Rushworth et al., 2012; Schultz, 2000). Notably, the eLPP is the only index here manifesting linearity in tracking the physical space of a stimulus, in contrast to the other indices associated with psychological interpretations of the physical world.

The lLPP also increases with fear intensity, but at a changing rate. At lower intensities, the rate is slow, and amplitudes for the bottom levels (2%, 15% and 21%) are essentially the same (p's $> .91$). At higher, consciously perceived, intensities (45% and potentially, 39%), lLPP amplitudes sharply accelerate. This profile fits closely a response curve characteristic of conscious object perception (Del Cul et al., 2007). As mentioned above, information processing at this late stage likely engages a distributed network (Adolphs, 2002; Vuilleumier, 2005). Indeed, the LPP component is linked to widely distributed sources in frontal and occipito-parietal regions (Carretie et al., 2006; Cuthbert et al., 2000b; Moratti et al., 2011). Particularly, the LPP is related to dynamic interaction between higher-order prefrontal cortex and lower-order visual cortex (Moratti et al., 2011). Combining EEG and functional magnetic resonance imaging (fMRI), recent work has specified a global network underpinning the LPP response to emotion, isolating visual cortices, amygdala, OFC and insula in emotion processing at this advanced stage (Liu et al., 2012; Sabatinelli et al., 2013; Sabatinelli et al., 2009). Therefore, as such long-range interactions and "global ignition" come online, conscious awareness of fear starts to emerge (Dehaene and Naccache, 2001; Lamme, 2010; Vuilleumier, 2005) and makes a very strong contribution (31%) to behavioral performance of fear detection.

In conclusion, current findings furnish some insights into the long-held multi-process view (Adolphs, 2002; LeDoux, 1995; Vuilleumier and Pourtois, 2007) and recent "multi-wave models" of emotion perception (Pessoa and Adolphs, 2010). By combining parametric signal manipulation, temporal resolution of ERP data, and psychophysical and neurometric analysis, we delineate the chronometry of four processes purportedly key to fear perception: As a fear-related stimulus projects its visual input to the retina, "quick-and-dirty" emotion categorization kicks off, followed by sensitive fear detection, then faithful valuation of fear intensity, and finally conscious awareness of fear in the perceiver. Lastly, to the extent that our labels of the psychological processes are conceptually constructed and somewhat arbitrary, future studies integrating psychophysics and neurometric analysis in other tasks and paradigms may further our understanding of the processes underlying the different ERP phases and components.

Conflict of interest

The authors declare no competing financial interests.

Acknowledgments

We thank David Rozek for assistance in experiment preparation and data collection, and Kevin Clancy for assistance with data analysis. This research was supported by the National Institute of Mental Health (R01MH093413 to W.L.).

References

Adolphs, R., 2002. Recognizing emotion from facial expressions: psychological and neurological mechanisms. Behav. Cogn. Neurosci. Rev. 1 (1), 21–62.
Amaral, D.G., Price, J.L., Pitkanen, A., Carmichael, S.T., 1992. Anatomical Organization of the Primate Amygdaloid Complex. Wiley-Liss, New York.
Amting, J.M., Greening, S.G., Mitchell, D.G., 2010. Multiple mechanisms of consciousness: the neural correlates of emotional awareness. J. Neurosci. 30 (30), 10039–10047. http://dx.doi.org/10.1523/JNEUROSCI.6434-09.2010.
Barrett, L.F., Bar, M., 2009. See it with feeling: affective predictions during object perception. Philos. Trans. R. Soc. Lond. B Biol. Sci. 364 (1521), 1325–1334, doi:364/1521/1325 [pii]10.1098/rstb.2008.0312.
Bell, A.J., Sejnowski, T.J., 1995. An information-maximization approach to blind separation and blind deconvolution. Neural Comput. 7 (6), 1129–1159.
Breiter, H.C., Etcoff, N.L., Whalen, P.J., Kennedy, W.A., Rauch, S.L., Buckner, R.L., Rosen, B.R., 1996. Response and habituation of the human amygdala during visual processing of facial expression. Neuron 17 (5), 875–887.
Brosch, T., Pourtois, G., Sander, D., 2010. The perception and categorisation of emotional stimuli: a review. Cogn. Emot. 24, 377–400.
Brosch, T., Pourtois, G., Sander, D., Vuilleumier, P., 2011. Additive effects of emotional, endogenous, and exogenous attention: behavioral and electrophysiological evidence. Neuropsychologica 49, 1779–1787.
Carretie, L., Hinojosa, J.A., Albert, J., Mercado, F., 2006. Neural response to sustained affective visual stimulation using an indirect task. Exp. Brain Res. 174 (4), 630–637. http://dx.doi.org/10.1007/s00221-006-0510-y.
Chikazoe, J., Lee, D.H., Kriegeskorte, N., Anderson, A.K., 2014. Population coding of affect across stimuli, modalities and individuals. Nat. Neurosci. 17 (8), 1114–1122. http://dx.doi.org/10.1038/nn.3749.
Christie, I.C., Friedman, B.H., 2004. Autonomic specificity of discrete emotion and dimensions of affective space: a multivariate approach. Int. J. Psychophysiol. 51 (2), 143–153.
Cuthbert, B.N., Schupp, H.T., Bradley, M.M., Birbaumer, N., Lang, P.J., 2000a. Brain potentials in affective picture processing: covariation with autonomic arousal and affective report. Biol. Psychol. 52 (2), 95–111.
Cuthbert, B.N., Schupp, H.T., Bradley, M.M., Birbaumer, N., Lang, P.J., 2000b. Brain potentials in affective picture processing: covariation with autonomic arousal and affective report. Biol. Psychol. 52 (2), 95–111.
Davis, M., Whalen, P.J., 2001. The amygdala: vigilance and emotion. Mol. Psychiatry 6 (1), 13–34.
Dehaene, S., Naccache, L., 2001. Towards a cognitive neuroscience of consciousness: basic evidence and a workspace framework. Cognition 79 (1–2), 1–37.
Del Cul, A., Baillet, S., Dehaene, S., 2007. Brain dynamics underlying the nonlinear threshold for access to consciousness. PLoS Biol. 5 (10), e260.
Delorme, A., Makeig, S., 2004. EEGLAB: an open source toolbox for analysis of single-trial EEG dynamics including independent component analysis. J. Neurosci. Methods 134 (1), 9–21. http://dx.doi.org/10.1016/j.jneumeth.2003.10.009.
Ekman, P., 1992. Are there basic emotions? Psychol. Rev. 99 (3), 550–553.
Forscher, E.C., Li, W., 2012. Hemispheric asymmetry and visuo-olfactory integration in perceiving subthreshold (micro) fearful expressions. J. Neurosci. 32 (6), 2159–2165. http://dx.doi.org/10.1523/JNEUROSCI.5094-11.2012.
Goldstone, R.L., Hendrickson, A.T., 2010. Categorical perception. Wiley Interdiscip. Rev. Cogn. Sci. 1 (1), 69–78. http://dx.doi.org/10.1002/wcs.26.
Hamann, S., 2012. What can neuroimaging meta-analyses really tell us about the nature of emotion? Behav. Brain Sci. 35 (3), 150–152. http://dx.doi.org/10.1017/S0140525X11001701.
Harris, L.R., Herpers, R., Jenkin, M., Allison, R.S., Jenkin, H., Kapralos, B., Felsner, S., 2012a. The relative contributions of radial and laminar optic flow to the perception of linear self-motion. J. Vis. 12 (10), 7. http://dx.doi.org/10.1167/12.10.7.
Harris, R.J., Young, A.W., Andrews, T.J., 2012b. Morphing between expressions dissociates continuous from categorical representations of facial expression in the human brain. Proc. Natl. Acad. Sci. USA 109 (51), 21164–21169. http://dx.doi.org/10.1073/pnas.1212207110.
Harris, R.J., Young, A.W., Andrews, T.J., 2014. Dynamic stimuli demonstrate a categorical representation of facial expression in the amygdala. Neuropsychologia 56, 47–52. http://dx.doi.org/10.1016/j.neuropsychologia.2014.01.005.
Helfman, G.S., 1989. Threat-sensitive predator avoidance in damselfish-trumpetfish interactions. Behav. Ecol. Sociobiol. 24 (1), 47–58. http://dx.doi.org/10.1007/Bf00300117.
Jemel, B., Schuller, A.M., Cheref-Khan, Y., Goffaux, V., Crommelinck, M., Bruyer, R., 2003. Stepwise emergence of the face-sensitive N170 event-related potential component. Neuroreport 14 (16), 2035–2039. http://dx.doi.org/10.1097/01.wnr.0000092465.31470.2f.
Johnson, M.H., 2005. Subcortical face processing. Nat. Rev. Neurosci. 6 (10), 766–774. http://dx.doi.org/10.1038/nrn1766.

Keil, A., Bradley, M.M., Hauk, O., Rockstroh, B., Elbert, T., Lang, P.J., 2002. Large-scale neural correlates of affective picture processing. Psychophysiology 39 (5), 641–649. http://dx.doi.org/10.1017/S0048577202394162.
Klein, S.A., 2001. Measuring, estimating, and understanding the psychometric function: a commentary. Percept. Psychophys. 63 (8), 1421–1455.
Krusemark, E.A., Li, W., 2013. From early sensory specialization to later perceptual generalization: dynamic temporal progression in perceiving individual threats. J. Neurosci. 33 (2), 587–594. http://dx.doi.org/10.1523/JNEUROSCI.1379-12.2013.
Lamme, V.A., 2010. How neuroscience will change our view on consciousness. Cogn. Neurosci. 1 (3), 204–220. http://dx.doi.org/10.1080/17588921003731586.
LeDoux, J.E., 1995. Emotion: clues from the brain. Annu. Rev. Psychol. 46, 209–235.
LeDoux, J.E., 2014. Coming to terms with fear. Proc. Natl. Acad. Sci. USA 111 (8), 2871–2878. http://dx.doi.org/10.1073/pnas.1400335111.
LeDoux, J.E., 2015. Anxious: Using the Brain to Understand and Treat Fear and Anxiety. Viking, New York, US.
Li, W., 2014. Learning to smell danger: acquired associative representation of threat in the olfactory cortex. Front. Behav. Neurosci. 8, 98. http://dx.doi.org/10.3389/fnbeh.2014.00098.
Li, W., Howard, J.D., Parrish, T.B., Gottfried, J.A., 2008. Aversive learning enhances perceptual and cortical discrimination of indiscriminable odor cues. Science 319 (5871), 1842–1845. http://dx.doi.org/10.1126/science.1152837.
Liu, Y., Huang, H., McGinnis-Deweese, M., Keil, A., Ding, M., 2012. Neural substrate of the late positive potential in emotional processing. J. Neurosci. 32 (42), 14563–14572. http://dx.doi.org/10.1523/JNEUROSCI.3109-12.2012.
Lundqvist, D., Flykt, A., Öhman, A., 1998. The Karolinska Directed Emotional Faces. Karolinska Institute, Psychology Section, Department of Clinical Neuroscience, Stockholm.
Luo, W.B., Feng, W.F., He, W.Q., Wang, N.Y., Luo, Y.J., 2010. Three stages of facial expression processing: ERP study with rapid serial visual presentation. NeuroImage 49, 1857–1867.
Mathews, A., Mackintosh, B., 1998. A cognitive model of selective processing in anxiety. Cogn. Ther. Res. 22 (6), 539–560.
Maren, S., 2016. Parsing reward and aversion in the amygdala. Neuron 90 (2), 209–211.
Miskovic, V., Keil, A., 2012. Acquired fears reflected in cortical sensory processing: a review of electrophysiological studies of human classical conditioning. Psychophysiology 49 (9), 1230–1241. http://dx.doi.org/10.1111/j.1469–8986.2012.01398.x.
Mitchell, D.G., Greening, S.G., 2012. Conscious perception of emotional stimuli: brain mechanisms. Neuroscientist 18 (4), 386–398. http://dx.doi.org/10.1177/1073858411416515.
Moratti, S., Saugar, C., Strange, B.A., 2011. Prefrontal-occipitoparietal coupling underlies late latency human neuronal responses to emotion. J. Neurosci. 31 (47), 17278–17286. http://dx.doi.org/10.1523/JNEUROSCI.2917-11.2011.
Mormann, F., Dubois, J., Kornblith, S., Milosavljevic, M., Cerf, M., Ison, M., Koch, C., 2011. A category-specific response to animals in the right human amygdala. Nat. Neurosci. 14 (10), 1247–1249. http://dx.doi.org/10.1038/nn.2899.
Morris, J.S., Frith, C.D., Perrett, D.I., Rowland, D., Young, A.W., Calder, A.J., Dolan, R.J., 1996. A differential neural response in the human amygdala to fearful and happy facial expressions. Nature 383 (6603), 812–815. http://dx.doi.org/10.1038/383812a0.
Nolan, H., Whelan, R., Reilly, R.B., 2010. FASTER: fully automated statistical thresholding for EEG artifact rejection. J. Neurosci. Methods 192 (1), 152–162. http://dx.doi.org/10.1016/j.jneumeth.2010.07.015.
O'Neill, M., Schultz, W., 2010. Coding of reward risk by orbitofrontal neurons is mostly distinct from coding of reward value. Neuron 68 (4), 789–800. http://dx.doi.org/10.1016/j.neuron.2010.09.031.
Ohman, A., 2005. The role of the amygdala in human fear: automatic detection of threat. Psychoneuroendocrinology 30 (10), 953–958.
Olofsson, J.K., Nordin, S., Sequeira, H., Polich, J., 2008. Affective picture processing: an integrative review of ERP findings. Biol. Psychol. 77 (3), 247–265. http://dx.doi.org/10.1016/j.biopsycho.2007.11.006.
Olofsson, J.K., Polich, J., 2007. Affective visual event-related potentials: arousal, repetition, and time-on-task. Biol. Psychol. 75 (1), 101–108. http://dx.doi.org/10.1016/j.biopsycho.2006.12.006.
Padmala, S., Pessoa, L., 2008. Affective learning enhances visual detection and responses in primary visual cortex. J. Neurosci. 28 (24), 6202–6210, doi:28/24/6202 [pii]10.1523/JNEUROSCI.1233-08.2008.
Pessoa, L., Adolphs, R., 2010. Emotion processing and the amygdala: from a 'low road' to 'many roads' of evaluating biological significance. Nat. Rev. Neurosci. 11 (11), 773–783. http://dx.doi.org/10.1038/nrn2920.
Phelps, E.A., LeDoux, J.E., 2005. Contributions of the amygdala to emotion processing: from animal models to human behavior. Neuron 48 (2), 175–187.
Pourtois, G., Grandjean, D., Sander, D., Vuilleumier, P., 2004. Electrophysiological correlates of rapid spatial orienting towards fearful faces. Cereb. Cortex 14, 619–633.
Riesenhuber, M., Poggio, T., 1999. Hierarchical models of object recognition in cortex. Nat. Neurosci. 2, 1019–1025.
Rushworth, M.F., Kolling, N., Sallet, J., Mars, R.B., 2012. Valuation and decision-making in frontal cortex: one or many serial or parallel systems? Curr. Opin. Neurobiol. 22 (6), 946–955. http://dx.doi.org/10.1016/j.conb.2012.04.011.
Russell, J.A., 1980. A circumplex model of affect. J. Personal. Soc. Psychol. 39 (6), 1161–1178. http://dx.doi.org/10.1037/h0077714.
Russell, J.A., 2003. Core affect and the psychological construction of emotion. Psychol. Rev. 110 (1), 145–172.
Sabatinelli, D., Keil, A., Frank, D.W., Lang, P.J., 2013. Emotional perception: correspondence of early and late event-related potentials with cortical and subcortical functional MRI. Biol. Psychol. 92 (3), 513–519. http://dx.doi.org/10.1016/j.biopsycho.2012.04.005.
Sabatinelli, D., Lang, P.J., Bradley, M.M., Costa, V.D., Keil, A., 2009. The timing of emotional discrimination in human amygdala and ventral visual cortex. J. Neurosci. 29 (47), 14864–14868. http://dx.doi.org/10.1523/JNEUROSCI.3278-09.2009.
Sacco, T., Sacchetti, B., 2010. Role of secondary sensory cortices in emotional memory storage and retrieval in rats. Science 329 (5992), 649–656. http://dx.doi.org/10.1126/science.1183165.
Schacter, D.L., Gilbert, D.T., Wegner, D.M., 2011. Psychology, 2nd ed. Worth, New York.
Schultz, W., 2000. Multiple reward signals in the brain. Nat. Rev. Neurosci. 1 (3), 199–207. http://dx.doi.org/10.1038/35044563.
Schupp, H.T., Cuthbert, B.N., Bradley, M.M., Cacioppo, J.T., Ito, T., Lang, P.J., 2000. Affective picture processing: the late positive potential is modulated by motivational relevance. Psychophysiology 37 (2), 257–261.
Serre, T., Oliva, A., Poggio, T., 2007. A feedforward architecture accounts for rapid categorization. Proc. Natl. Acad. Sci. USA 104 (15), 6424–6429.
Tamietto, M., de Gelder, B., 2010. Neural bases of the non-conscious perception of emotional signals. Nat. Rev. Neurosci. 11 (10), 697–709. http://dx.doi.org/10.1038/nrn2889.
Vuilleumier, P., 2005. How brains beware: neural mechanisms of emotional attention. Trends Cogn. Sci. 9 (12), 585–594. http://dx.doi.org/10.1016/j.tics.2005.10.011.
Vuilleumier, P., Armony, J.L., Driver, J., Dolan, R.J., 2003. Distinct spatial frequency sensitivities for processing faces and emotional expressions. Nat. Neurosci. 6 (6), 624–631.
Vuilleumier, P., Pourtois, G., 2007. Distributed and interactive brain mechanisms during emotion face perception: evidence from functional neuroimaging. Neuropsychologia 45 (1), 174–194, doi:S0028-3932(06)00229-6 [pii] 10.1016/j.neuropsychologia.2006.06.003.
Weinberger, N.M., 2007. Associative representational plasticity in the auditory cortex: a synthesis of two disciplines. Learn. Mem. 14 (1–2), 1–16.
Wichmann, F.A., Hill, N.J., 2001. The psychometric function: I. Fitting, sampling, and goodness of fit. Percept. Psychophys. 63 (8), 1293–1313.
You, Y., Li, W., 2016. Parallel processing of general and specific threat during early stages of perception. Soc. Cogn. Affect. Neurosci. 11 (3), 395–404. http://dx.doi.org/10.1093/scan/nsv123.
Young, A.W., Rowland, D., Calder, A.J., Etcoff, N.L., Seth, A., Perrett, D.I., 1997. Facial expression megamix: tests of dimensional and category accounts of emotion recognition. Cognition 63 (3), 271–313.
Zwislocki, J.J., Relkin, E.M., 2001. On a psychophysical transformed-rule up and down method converging on a 75% level of correct responses. Proc. Natl. Acad. Sci. USA 98 (8), 4811–4814. http://dx.doi.org/10.1073/pnas.081082598.